

# Effect of alkalinity on the hydrothermal synthesis of $\text{Li}_2\text{ZrO}_3$ nanotube arrays

Limin Guo · Xiaohui Wang · Shaopeng Zhang ·  
Caifu Zhong · Longtu Li

Received: 23 March 2011 / Accepted: 25 May 2011 / Published online: 4 June 2011  
© Springer Science+Business Media, LLC 2011

**Abstract** High aspect-ratio  $\text{Li}_2\text{ZrO}_3$  nanotube (NT) layers were obtained by hydrothermal synthesis in  $\text{LiOH}$  solution using anodic  $\text{ZrO}_2$  NT arrays as templates. Characterizations of SEM, XRD, and TEM were performed. The results showed that tetragonal  $\text{Li}_2\text{ZrO}_3$  NTs arrays containing a little monoclinic  $\text{ZrO}_2$  can be obtained using this simple method. The mean diameter of the NTs is approximately 150 nm. The alkalinity of hydrothermal solution was proved to have significant effect on the formation of the  $\text{Li}_2\text{ZrO}_3$  NT arrays. Under different alkalinity, different growth mechanisms dominated the formation of the nanotubular layers.

## Introduction

In recent years,  $\text{Li}_2\text{ZrO}_3$  ceramics have been extensively studied for their applications as electronic devices in batteries and breeder materials for nuclear fusion reactors [1, 2]. Moreover,  $\text{Li}_2\text{ZrO}_3$  is a promising candidate for  $\text{CO}_2$  sorption at high temperature [3, 4]. Separation of  $\text{CO}_2$  is a significant industrial technology in a lot of fields such as enhancing oil recovery, preparing hydrogen from methanol or methane, etc. [5, 6]. The main challenge is to find a  $\text{Li}_2\text{ZrO}_3$  acceptor with fast kinetics, excellent capture capacity and structure stability under the high working temperature. As we know, the microstructure can influence the performance of some materials. Therefore, synthesis of  $\text{Li}_2\text{ZrO}_3$  ceramic with nano-scaled size has become a promising research field [7–9].

Comparing to the nanoparticle-shape  $\text{Li}_2\text{ZrO}_3$ , the nanotubular arrays would be more proper for  $\text{CO}_2$  absorbent due to their large surface area, improved kinetic property and high regeneration ratio. In addition, the agglomeration and losing of porosity could be prevented during the regeneration process for the  $\text{Li}_2\text{ZrO}_3$  nanotubes (NTs) acceptor. As we know, a higher temperature (above 700 °C) is generally requested for the regeneration of  $\text{Li}_2\text{ZrO}_3$  from  $\text{Li}_2\text{CO}_3$ . And the agglomeration of particles is inevitable during the sorption–desorption cycles [10]. The  $\text{Li}_2\text{ZrO}_3$  layers with a NT array configuration would be more stable in this process.

As reported, solid-state reaction is the most common synthesis route for the  $\text{Li}_2\text{ZrO}_3$  ceramic. However, a high temperature (850–1000 °C) and long reaction time is usually required [11]. And it is difficult to control the particles size. Therefore, preparation of nano-scaled  $\text{Li}_2\text{ZrO}_3$ , especially those with nanotubular structure remains a challenge in the materials science. The hydrothermal method is known for the controllable synthesis route of high-purity materials at low temperatures [12, 13]. Up to now, the formation of barium titanate [14] and barium strontium titanate [15] NTs by hydrothermal reaction have been well studied. But little reports focus on the in situ synthesis of  $\text{Li}_2\text{ZrO}_3$  NTs. In this article, we employed anodized  $\text{ZrO}_2$  NTs as templates to prepare the  $\text{Li}_2\text{ZrO}_3$  NT arrays on Zr substrates by hydrothermal route. In order to thoroughly understand the growth mechanism, different hydrothermal conditions were used. This work is helpful for preparation of other zirconate NTs in the future.

L. Guo · X. Wang (✉) · S. Zhang · C. Zhong · L. Li  
State Key Laboratory of New Ceramics and Fine Processing,  
Department of Materials Science and Engineering,  
Tsinghua University, Beijing 100084, China  
e-mail: wxh@mail.tsinghua.edu.cn

## Experiments

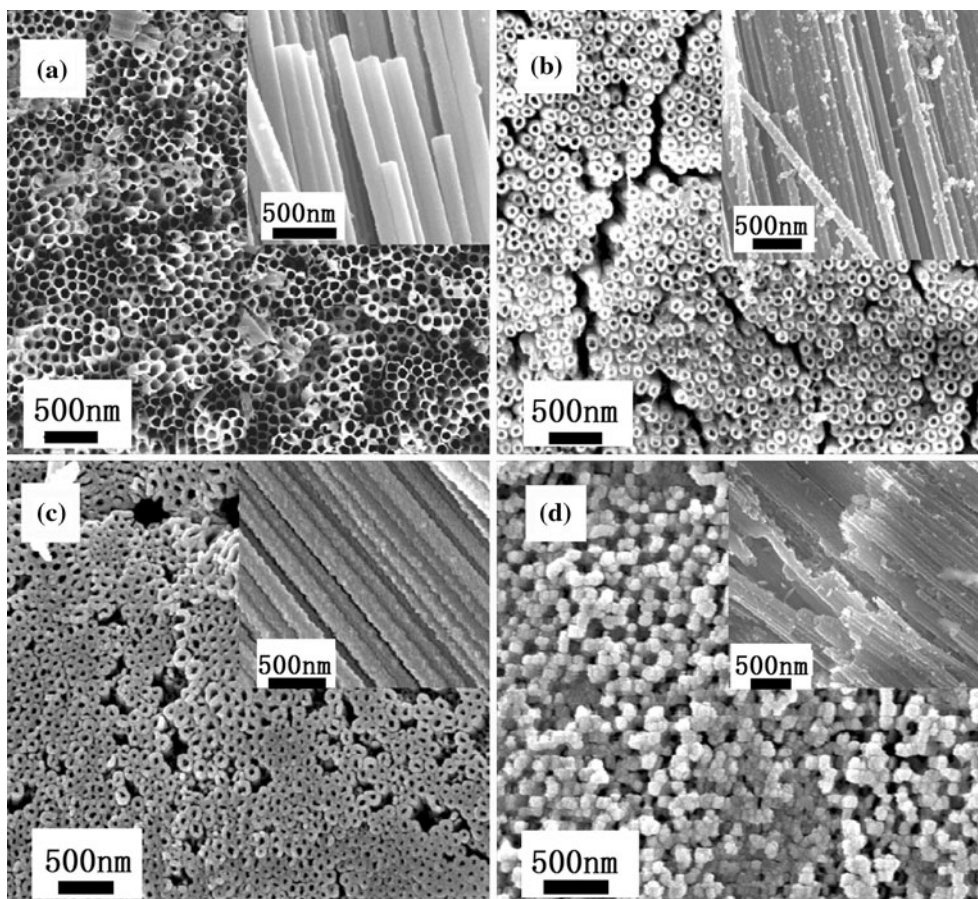
Zirconium foils (10 × 7 × 0.5 mm) with a purity of 99.7% were used for anodization to obtain  $\text{ZrO}_2$  NT

arrays. Electrolytes in the anodizing process were formamide and glycerol (GE) (volume ratio 1:1) containing 0.5 wt% NH<sub>4</sub>F. The anodization details could be found in our early study [16]. The as-synthesis ZrO<sub>2</sub> NT layers were annealed at 400 °C for 3 h to obtain a crystalline structure [16]. Then the samples were held in the center of Teflon reaction vessels. The LiOH solutions prepared by CO<sub>2</sub>-free deionized water filled to 70% of the vessels. Then, the hydrothermal vessels were placed into an oven heated to 200 °C, and holding this temperature for 4 h. Finally, the samples were removed out, rinsed in CO<sub>2</sub>-free deionized water and dried. For comparison, LiOH solution with concentrations of 0.01, 0.05, 0.1, and 0.5 M were used under the same hydrothermal conditions mentioned above.

Microstructure of the NTs was observed by a field emission scanning electron microscope (FESEM, LEO-1530, LEO, Oberkochen, Germany). The cross-section images and selected area electron diffraction (SAED) patterns were obtained by a high resolution transmission electron microscope (HRTEM, JEOL-2010, Japan). Crystal structures of the specimens were determined by X-ray diffraction (XRD 2500, Rigaku, Tokyo, Japan).

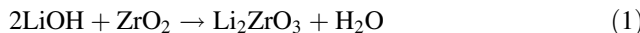
## Results and discussion

Figure 1a shows the FESEM image of the as-prepared ZrO<sub>2</sub> templates anodic grown on Zr substrates. The layers consist of highly ordered NT arrays with an open porous structure at the top end. The diameters of the NTs range from 150 to 200 nm with smooth and straight walls (inset of Fig. 1a). Figure 1b, c, d show the FESEM images of the NT arrays obtained after hydrothermal treatment of ZrO<sub>2</sub> templates in solutions with different LiOH concentration. At a lower LiOH concentration (0.01 M), no distinct changes can be found on the samples. Morphology of the layers is nearly the same to the as-prepared ZrO<sub>2</sub> NTs arrays (SEM images are omitted). Minor differences are revealed for the samples obtained in 0.05 M LiOH solutions (Fig. 1b). The tubal wall becomes a little thicker and a quantity of particles is attached on the outer side of the walls. After hydrothermal treatment of the templates in 0.1 M LiOH solutions, an ordered porous structure still existed in the layer. But evident distinctions are displayed. The wall of the NTs becomes thicker and the spacing between NTs is not apparent (Fig. 1c). It could be explained by the crystal cell expansion during the in situ



**Fig. 1** SEM images of anodized ZrO<sub>2</sub> NTs (a), and ZrO<sub>2</sub> templates after hydrothermal reaction in 0.05 M (b), 0.1 M (c), and 0.5 M (d) LiOH solution at 200 °C for 4 h

formation of  $\text{Li}_2\text{ZrO}_3$  NTs [14, 15].  $\text{Li}^+$  are transmitted into zirconia lattice and react with the templates by the assisting of high temperature and pressure in hydrothermal vessel. The reaction formulation is as follow:



With addition of 0.5 M LiOH in hydrothermal vessels, the obtained NT arrays collapse severely on the walls and the surface of the layer is overlaid by nano-scaled particles. Only a few pores can be found under the grainy layer (Fig. 1d). This is not favorable on their application for the un-stability and low porosity.

X-ray diffraction patterns of the as-synthesized materials under different alkalinity are shown in Fig. 2. Diffraction peaks marked with triangles in the patterns can be assigned to the tetragonal  $\text{Li}_2\text{ZrO}_3$  with some indication of other crystalline by-products such as lithium carbonate (marked with tetragons) or monoclinic  $\text{ZrO}_2$  remain (marked with rotundities). Evidently, the intensity of the peaks for crystalline  $\text{Li}_2\text{ZrO}_3$  increases along with the enhancing of hydrothermal alkalinity (Fig. 2a: 0.01 M, b: 0.05 M, c: 0.1 M, and d: 0.5 M). A fairly pure  $\text{Li}_2\text{ZrO}_3$  NTs layer can be obtained in the solutions with LiOH concentrations above 0.1 M. However, the higher alkalinity (0.1 and 0.5 M) gives rise to the formation of  $\text{Li}_2\text{CO}_3$  impurity in the layers. Weak peaks for monoclinic  $\text{ZrO}_2$  indicate a little partial  $\text{ZrO}_2$  remain in the templates.

The results presented above suggest that  $\text{Li}_2\text{ZrO}_3$  NT arrays can be achieved by hydrothermal reaction of  $\text{ZrO}_2$  NTs and LiOH solutions. The content of  $\text{Li}_2\text{ZrO}_3$  in the layers increases with the hydrothermal alkalinity (0.01–0.5 M LiOH). But the ordered porous structure would be

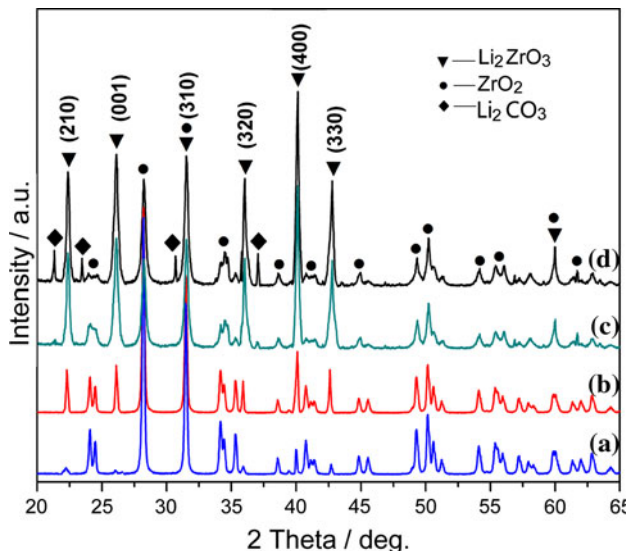


**Fig. 2** XRD patterns of the as-prepared NTs arrays obtained in 0.01 M (a), 0.05 (b), 0.1 M (c), and 0.5 M (d) LiOH solution at 200 °C for 4 h

damaged under the LiOH concentration higher than 0.1 M. Considering both the purity and morphology of the obtained layer, 0.1 M LiOH solution is preferable to the synthesis of the  $\text{Li}_2\text{ZrO}_3$  NT arrays. TEM observation is also performed on the specimens obtained in 0.1 M LiOH solution. In contrast to the as-prepared  $\text{ZrO}_2$  NT (inset of Fig. 3a), the  $\text{Li}_2\text{ZrO}_3$  NT gets thicker and rougher after hydrothermal reactions (Fig. 3a). This agrees well with the SEM images. Fig. 3b shows the HRTEM image and SAED patterns of an isolated  $\text{Li}_2\text{ZrO}_3$  NT. The diffraction spots (inset of Fig. 3b) provide evidence that the isolated  $\text{Li}_2\text{ZrO}_3$  NT has a single crystal structure. The  $d$  spacing estimated from the lattice fringes of the HRTEM pattern is about 0.33 nm (Fig. 3b),

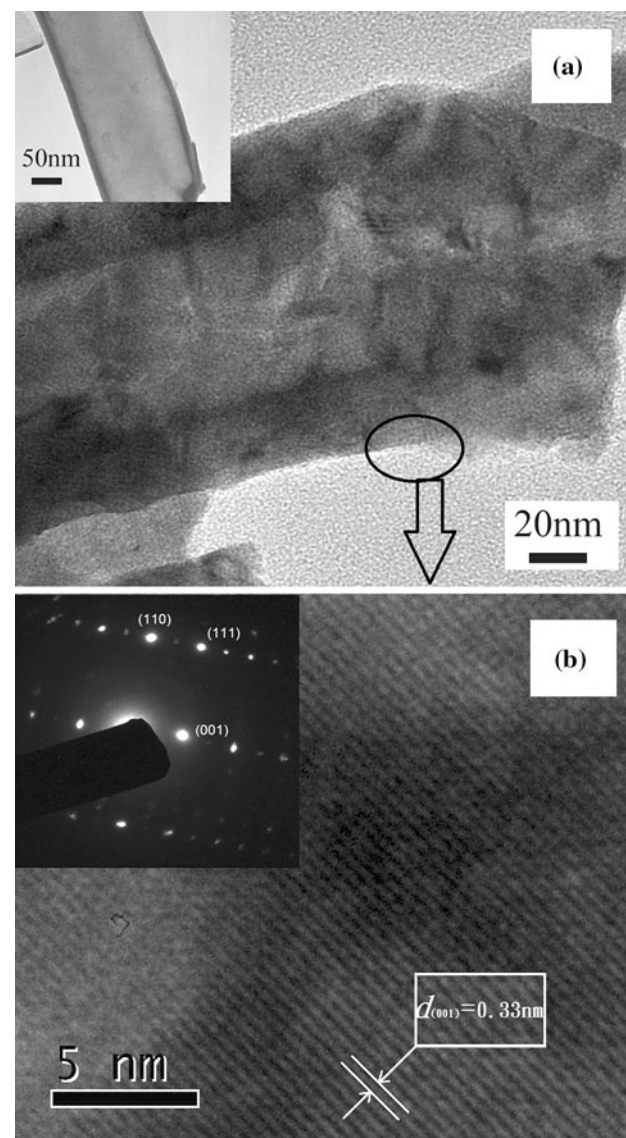


**Fig. 3** **a** TEM images of  $\text{Li}_2\text{ZrO}_3$  NT obtained in 0.1 M LiOH solution (with anodized  $\text{ZrO}_2$  NT in the inset), and HRTEM images of (a), inset corresponding SAED pattern

which is close to the {001} inter-planar spacing of tetragonal  $\text{Li}_2\text{ZrO}_3$  crystal, 0.34 nm (PDF Card No. 20-647).

Deduced from the experimental results, two mechanisms can be used to explain the synthesis of the  $\text{Li}_2\text{ZrO}_3$  NTs: in situ mechanism and dissolution-precipitation process as seen in Fig. 4. In the initial stage of the hydrothermal treatment, the dispersed  $\text{Li}^+$  ions concentrate around the  $\text{ZrO}_2$  NTs arrays (Fig. 4a). Partial supersaturated  $\text{Li}^+$  ions enter the crystal lattice of  $\text{ZrO}_2$  under high pressure and form a tetragonal  $\text{Li}_2\text{ZrO}_3$  NTs (Fig. 4b). During this in situ growth process, the NTs walls become thicker and rougher due to the crystal cell expansion. However, for the blocking of the outer tubal walls, especially on the compact position (root of the NT or bottom barrier layer) of the layer,  $\text{Li}^+$  ions are deficient and segmental  $\text{ZrO}_2$  template remains (Fig. 4b, c). Accompanying with the formation of  $\text{Li}_2\text{ZrO}_3$  NTs, little portion of  $\text{ZrO}_2$  is dissolved in the alkaline solution assisted by the high temperature and pressure. When  $\text{ZrO}^{2+}$  and  $\text{Zr}^{4+}$  are introduced into the solution,  $\text{Li}^+$  are combined with the  $\text{ZrO}^{2+}$  or  $\text{Zr}^{4+}$  and agglomerate on the heterogeneous-nucleation sites provided by the NT arrays. Herein, the grainy  $\text{Li}_2\text{ZrO}_3$  is formed on or in the already-formed  $\text{Li}_2\text{ZrO}_3$  NTs (Fig. 4c). This dissolution-precipitation process is mainly involved

with the alkalinity of the hydrothermal solution [17]. With addition of  $\text{LiOH}$  concentration (0.5 M), the dissolution rate of  $\text{ZrO}_2$  is elevated. The NT layers collapse severely under the same hydrothermal time and temperature (Fig. 1d). This destructive process is unfavorable for the formation and application of the  $\text{Li}_2\text{ZrO}_3$  NT layers. Consequently, in order to in situ growth  $\text{Li}_2\text{ZrO}_3$  NTs arrays under a certain reaction time and temperature, avoid the deposition of  $\text{Li}_2\text{ZrO}_3$  particles on the surface of the already-formed layers, suitable hydrothermal alkalinity should be applied.

## Conclusions

Using anodic  $\text{ZrO}_2$  NTs arrays as templates,  $\text{Li}_2\text{ZrO}_3$  NTs arrays have been obtained by hydrothermal synthesis in alkaline solutions ( $\text{LiOH}$ ). The alkalinity of the hydrothermal solution has significant effect on the growth mechanism of  $\text{Li}_2\text{ZrO}_3$ . At a lower alkalinity, the in situ formation is dominant in the reactions. The addition of  $\text{LiOH}$  concentration results in the dissolution of  $\text{ZrO}_2$  and formation of  $\text{Li}_2\text{ZrO}_3$  particles on the surface of the  $\text{Li}_2\text{ZrO}_3$  NTs. For synthesis of  $\text{Li}_2\text{ZrO}_3$  layers with NTs structure, proper alkalinity should be adopted in the hydrothermal reactions.

**Acknowledgements** The study was supported by National Science fund for distinguished young scholars (Grant No. 50625204), Science Fund for Creative Research Groups (Grant No. 50921061), Ministry of Sciences and Technology of China through National Basic Research Program of China (973 Program 2009CB623301), outstanding tutors for doctoral dissertations of S&T project in Beijing (No. YB20081000302), and Tsinghua University Initiative Scientific Research Program.

## References

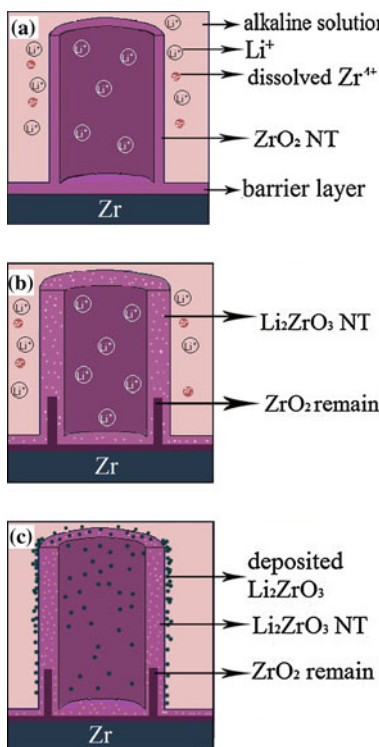


**Fig. 4** Growth mechanism of  $\text{Li}_2\text{ZrO}_3$  NT by hydrothermal method in  $\text{LiOH}$  solution. **a, b** The supersaturated  $\text{Li}^+$  ions enter the crystal lattice of  $\text{ZrO}_2$  and form a tetragonal  $\text{Li}_2\text{ZrO}_3$  structure. **c** Partially dissolved  $\text{Zr}^{4+}$  ions react with the superfluous  $\text{Li}^+$  ions and form tiny  $\text{Li}_2\text{ZrO}_3$  particles on the top and wall of the already-formed NT

- Nishikawa M, Baba AJ (1998) Nucl Mater 257:162
- Kinjyo T, Nishikawa M, Enoda M, Fukada S (2008) Fusion Eng Des 83:580
- Ochoa-Fernandez E, Ronning M, Grande T, Chen D (2006) Chem Mater 18:6037
- Ida J, Xiong RT, Lin YS (2004) Sep Purif Technol 36:41
- Harrison DP (2008) Ind Eng Chem Res 47:6486
- Yang H, Xu Z, Fan M et al (2008) J Environ Sci 20:14
- Kang SZ, Wu T, Li X, Mu J (2010) Mater Lett 64:1404
- Nair BN, Yamaguchi T, Kawamura H, Nakao SI (2004) J Am Ceram Soc E7(1):68
- Ochoa-Fernandez E, Ronning M, Yu X, Grande T, Chen D (2008) Ind Eng Chem Res 47:434
- Pfeiffer H, Bosch P (2005) Chem Mater 17:1704
- Yi KB, Eriksen DO (2006) Sep Sci Technol 41:283
- Chen X, Fan H, Liu L (2005) J Cryst Growth 284:434
- Walton RI (2002) Chem Soc Rev 31:230
- Padture NP, Wei X (2003) J Am Ceram Soc 86:2215
- Zhao J, Wang X, Chen R, Li L (2005) Mater Lett 59:2329
- Guo L, Zhao JL, Wang XX, Xu XW, Li YX (2009) Int J Appl Ceram Technol 6:636
- Yang Y, Wang X, Sun C, Yao G, Li L (2008) J Am Ceram Soc 91:3792